FATIGUE BEHAVIOR AND LIFE PREDICTIONS FOR AZ91E-T6 CAST MAGNESIUM ALLOY

R.I. STEPHENS, D.L. GOODENBERGER and
V.V. OGAREVIC
Mechanical Engineering Dept., The University of Iowa, Iowa City, IA USA
S.N. PEROV
Aircraft Dept., Samara Aviation Institute, Samara, Russia

ABSTRACT

Low cycle fatigue and fatigue crack growth behavior under constant amplitude loading were obtained for AZ91E-T6 cast magnesium alloy. Strain ratios, R, of 0, -1 and -2 were used for low cycle fatigue tests while load ratios, R, of 0.05 and 0.5 were used for fatigue crack growth tests. Variable amplitude fatigue tests with 41913 reversals per block were performed using keyhole compact type specimens. Significant mean stress relaxation occurred for higher strain amplitude R = 0 and -2 low cycle fatigue tests. The mean stress effects were analyzed using the Morrow and SWT models. Fatigue crack growth data were analyzed with and without crack closure. Fatigue crack growth was predominantly quasi-cleavage. Commercially available fatigue life calculation software was used to predict fatigue crack "initiation" life (1 mm crack) and subsequent fatigue crack growth life for the variable amplitude tests. Fatigue life predictions ranged from good to poor and from conservative to non-conservative.

KEYWORDS

Magnesium, low cycle fatigue, fatigue crack growth, variable amplitude, life predictions

INTRODUCTION

Fatigue behavior of magnesium alloys, other than S-N behavior, is not well documented, as indicated by Ogarevic and Stephens (1990) in their fatigue of magnesium alloys review paper. This research considers three different aspects of fatigue of AZ91E-T6 sand-cast magnesium alloy which is a material with stringent controls on Fe, Cu and Ni in order to provide improved corrosion resistance. The three areas of fatigue research were constant amplitude strain-controlled low cycle fatigue with strain ratios, R, equal to 0, -1 and -2, fatigue crack growth with load ratios, R, equal to 0.05 and 0.5, and variable amplitude loading life predictions. The composition of the material obtained from one heat is given in Table 1 and typical or average monotonic tensile properties are given in Table 2. These properties indicate a high quality material with both adequate strength and ductility.

Table 1. Composition for AZ91E-T6, weight percent

Mg	Al	Zn	Mn	Cu	Si	Fe	Ni
base	8.97	0.54	0.17	0.010	0.01	0.003	0.0010

LOW CYCLE FATIGUE

Low cycle fatigue tests were performed in strain control on 6.4 mm diameter smooth axial specimens using a triangular waveform with a frequency ranging from 0.5 to 30 Hz. Failure criteria were fracture or 20% drop in maximum tensile load. Fully-reversed, R = -1, low cycle fatigue behavior is shown in Fig. 1 where total, elastic and plastic strain amplitudes are plotted against number of reversals to failure, $2N_f$. Scatter is less than that observed in many strain-life curves, particularly for cast products. Elastic and plastic values were obtained at approximately half-life. Log-log regression results using

$$\frac{\Delta\varepsilon}{2} = \frac{\Delta\varepsilon_e}{2} + \frac{\Delta\varepsilon_p}{2} = \frac{\sigma_f'}{E}(2N_f)^b + \varepsilon_f'(2N_f)^c \qquad (1)$$

are given in Table 3. The R = -1 cyclic stress-strain properties in Table 3 were also based upon half-life values of stress and strains. The material cyclic strain hardens with approximately a 25% increase in cyclic yield strength over the monotonic yield strength. Half-life cyclic stress-strain data for both R = 0 and -2 agreed very favorably with the R = -1 results.

Fig. 2 is a superposition of the three R ratio strain-life results. Here it is evident that data for all three R ratios at large strain amplitudes are similar while at the smaller strain amplitudes the R = 0 strain tests indicate less fatigue resistance. At large strain amplitude, significant mean stress relaxation occurred due to substantial plasticity providing similar fatigue resistance. At the smaller strain amplitudes, with R = 0, higher mean tensile stress existed along with higher ratios of $\sigma_{mean}/\sigma_{max}$ and thus provided the lower fatigue resistance. Both the Morrow model, from Graham (1968) equation 2, and the Smith, Watson, Topper (1970) (SWT) model, equation 3, were used to analyze the axial strain-controlled mean stress effects.

$$\frac{\Delta\varepsilon}{2} = \frac{\sigma_f'-\sigma_m}{E}(2N_f)^b + \varepsilon_f'(2N_f)^c \qquad (2)$$

$$\sigma_{max}\varepsilon_a = \frac{(\sigma_f')^2}{E}(2N_f)^{2b} + \sigma_f'\varepsilon_f'(2N_f)^{b+c} \qquad (3)$$

Table 2. Monotonic Tensile Properties

Young's modulus, E [GPa]	45
0.2% yield strength, Sy [MPa]	142
Ultimate strength, S_u [MPa]	318
True fracture strength, σ_f [MPa]	356
Percent elongation, % El	12
Percent reduction in area, % RA	12.8
True fracture ductility, ε_f	0.137
Strain hardening exponent, n	618*
Strength coefficient, K [MPa]	0.248*

* Typical from one test specimen

Table 3. Low Cycle Fatigue and Cyclic Stress-Strain Properties

Fatigue strength coefficient, σ_f [MPa]	831
Fatigue strength exponent, b	-0.148
Fatigue ductility coefficient, ε_f'	0.089
Fatigue ductility exponent, c	-0.451
Cyclic yield strength, S_y' [MPa]	180
Cyclic strength coefficient, K' [MPa]	552
Cyclic strain-hardening exponent, n'	0.184

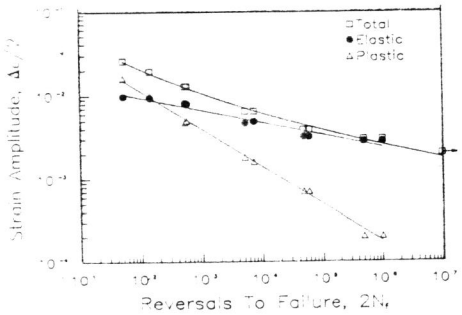

Fig. 1 Fully-Reversed (R = -1) Fatigue Behavior

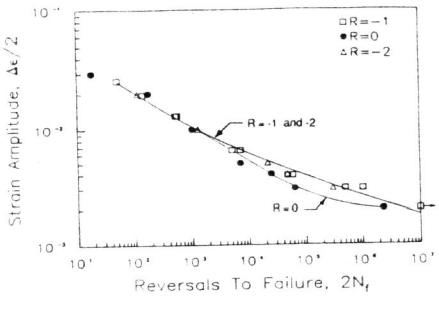

Fig. 2 Fatigue Behavior for all Strain Ratios

For the Morrow model, most predicted data fell within a factor of ± 2 while a few predictions fell outside this range and were non-conservative. For the SWT parameter, predictions were mostly non-conservative by a factor of 2 to 5. Thus the Morrow model slightly better described the mean stress effects.

FATIGUE CRACK GROWTH

Compact tension, C(T), specimens with H/W = 0.6 were used for fatigue crack growth testing. Crack length was measured optically with a 33x traveling microscope using stroboscopic illumination with frequencies varying from 20 to 40 Hz. Crack closure values were obtained with a COD gage attached at the crack mouth. The log-log linear region II da/dN - ΔK data were obtained under constant amplitude loading, while threshold region I data were obtained by load shedding. Region II fatigue crack growth data were reduced using an incremental polynominal while region I data were reduced using a finite difference secant method. These results are shown in Fig. 3 as da/dN versus applied ΔK for both R = 0.05 and 0.5. Here the solid data points represent R = 0.5 and the open data points represent R = 0.05. Scatter for R = 0.5 appears to be about a factor of 2 and for R = 0.05 less than a factor of 1.5. These ranges are not unusual for many materials. There is a small mean stress or R ratio effect in Region II which is also consistent with that for many materials. The Region II crack growth rate data were modeled using log-log linear regression of the Paris equation.

$$\frac{da}{dN} = A(\Delta K)^n \qquad (4)$$

Values of the Paris exponent, n, and coefficient, A, for each R ratio are given in Table 4. The values of these coefficients and exponents fall within ranges reported by Ogarevic and Stephens (1990) for several magnesium alloys. Final values of K_{max} at near fracture were about 9 to 10 MPa$\sqrt{m}$ for each R ratio as shown in Fig. 3.

Stress intensity factor threshold levels, ΔK_{th}, could only be obtained for R = 0.5. Using a log-log linear regression analysis of the data below 10^{-9} m/cycle and defining ΔK_{th} at 10^{-10} m/cycle, ΔK_{th} for R = 0.5 was 0.83 MPa$\sqrt{m}$. A ΔK_{th} value was not obtained for R = 0.05, because of lack of crack growth rate data less than 10^{-9} m/cycle. Based on data that were obtained, the value of ΔK_{th} for R = 0.05 will be $\leq$ 1.5 MPa$\sqrt{m}$. At near threshold R = 0.05 crack growth testing, the applied loads became very small (< 450 Newtons), and crack opening displacement was negligible. The crack tip could not be established by optical

means with any confidence. Although the values for ΔK_{th} are quite low when compared with most cast and wrought metals, they are within the range of values reported by Ogarevic and Stephens (1990) for several magnesium alloys.

To account for the effects of crack closure, as proposed by Elber (1970), the effective stress intensity factor, ΔK_{eff}, was used. To convert the applied stress intensity factor range, ΔK, to ΔK_{eff}, it was necessary to determine the crack opening load, P_{op}, from a plot of load versus COD. The effective load range is then given by

$$\Delta P_{eff} = P_{max} - P_{op} \qquad (5)$$

P_{op} was obtained at the tangent location of the upper portion of the load versus COD curve. For R = 0.05, P_{op}/P_{max} ranged from 0.32 to 0.42 in region I and from essentially zero to 0.17 in region II. No fatigue crack closure was noticed for the R = 0.5 testing, including the near threshold tests. This is not surprising since the crack would probably be open for the entire loading cycle due to the high tensile mean loads. Thus, $\Delta K_{eff} = \Delta K_{applied}$ for all R = 0.5 data. Fig. 4 is a plot of da/dN versus ΔK_{eff}. The R = 0.5 data are the same as in Fig. 3 due to the lack of crack closure for this load ratio. A comparison of Figures 3 and 4 shows that crack closure analysis has essentially eliminated the R ratio effect for most of Region II, since much of the R = 0.05 data falls within the scatterband of the R = 0.5 data. For the near threshold Region it is seen from Fig. 4 that using ΔK_{eff} has shifted the R = 0.05 data to the other side of the R = 0.5 Region I data. This may still be within the scatterband for the R = 0.5, but clearly points out the many problems associated with crack closure determination and usage. Fatigue crack growth parameters using ΔK_{eff} for R = 0.05 were $A = 4.7 \times 10^{-10}$, n = 3.7 and effective ΔK_{th} was ≤ 0.75 MPa$\sqrt{m}$.

Table 4. Fatigue Crack Growth Parameters (units m/cycle and MPa$\sqrt{m}$)

Load Ratio R	Paris Eqn. Coefficient A	Paris Eqn. Exponent n	ΔK_{th} MPa$\sqrt{m}$
0.05	1.8×10^{-10}	3.9	≤ 1.5
0.5	9.8×10^{-10}	3.3	0.83

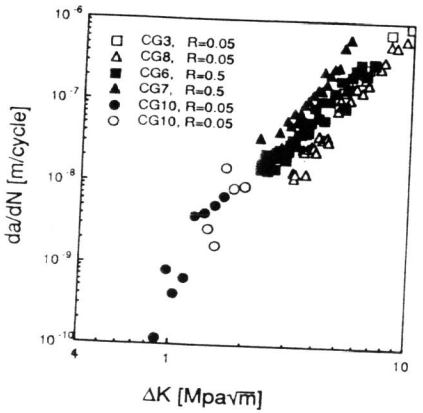

Fig. 3 da/dN versus Applied ΔK

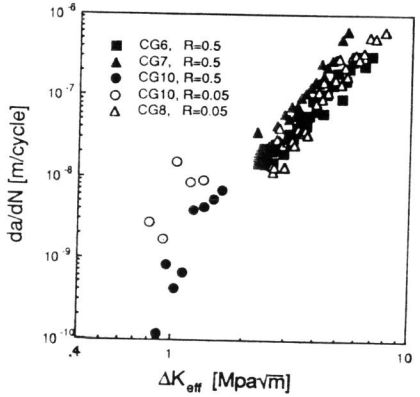

Fig. 4 da/dN versus Effective ΔK

For all fatigue crack growth tests, the macro fracture surface was flat and mode I. SEM fractography revealed substantial fretting in region I with R = 0.05 due to substantial crack closure. In region II, no clear striations were observed, however, quasi-cleavage fatigue crack growth fractures were observed.

VARIABLE AMPLITUDE LOADING

The purpose of this portion of the research was to determine the feasibility of applying commonly used fatigue life calculation models to AZ91E-T6 cast magnesium alloy. Experimental variable load amplitude tests were performed using the 8.2 mm thick keyhole notched specimen shown in Fig. 5. The keyhole notch was drilled and reamed and has a theoretical stress concentration factor of 3.4 as determined by finite element analysis by Lease and Stephens (1991). The load spectrum used was developed by Lease and Stephens (1991) and contained 41913 reversals with both positive and negative mean loads. The normalized load amplitude histogram, as obtained by rainflow counting, is shown in Fig. 6. The load spectrum was designed to have substantial cycles at the intermediate amplitude levels to better distribute fatigue damage. Three different peak load scaling factors were used with this normalized load spectrum in an attempt to produce comparably short, intermediate and long fatigue test lives. The three peak loads, 1, 2 and 3, resulted in nominal net stresses at the notch root of 97, 81 and 73 MPa respectively. The theoretical elastic stress at the notch root would be 3.4 times the nominal values or 330, 274 and 247

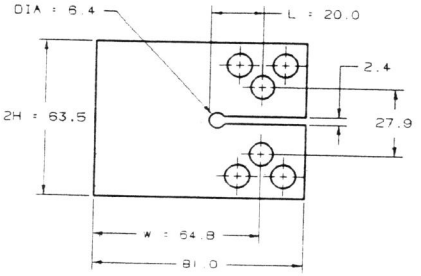

Fig. 5 Keyhole specimen
(all dimensions in mm)

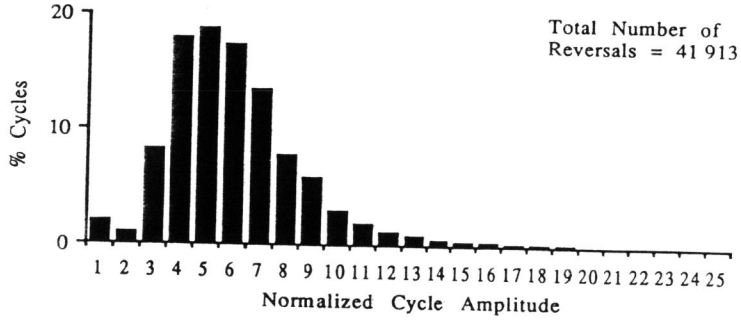

Fig. 6 Load Amplitude Histogram

MPa respectively. These values are greater than the 180 MPa cyclic yield strength given in Table 3, and hence local notch yielding existed in all tests. Fatigue cracks grown from the root of the keyhole notch were measured by a 33x traveling telescope. The formation of a surface crack of 1.0 mm was defined as fatigue crack "initiation". This value represents a realistically measurable value and is consistent with final crack sizes in LCF tests. Fatigue crack length readings were recorded from the first detectable surface crack to final fracture.

Experimental results of the variable amplitude fatigue tests are shown in Table 5. History blocks to fatigue crack initiation (surface crack of 1.0 mm), history blocks of fatigue crack growth (fatigue life from crack initiation to final fracture) and history blocks of total fatigue life (initiation life + growth life) are given for each test. A history block is defined as one complete pass through the 41913 reversal variable amplitude spectrum. A total of five test specimens were investigated. Tests at load levels 1 and 2 were duplicated with very reasonable scatter. The total number of reversals applied to each specimen varied from 1.7 x 10^5 to 2.0 x 10^6. Overall, experimental fatigue crack initiation life accounted for approximately 75 to 93% of the total fatigue life for each specimen. This means that crack initiation fatigue life calculations for this magnesium alloy, spectrum, and keyhole specimen are more important in comparison with crack growth fatigue life calculations. A large error in the calculations for crack initiation can cause a large error in life calculations even if the crack growth life calculations were very accurate.

Table 5. Experimental Results of Variable Amplitude Fatigue Testing

Load Level	Total Life, Blocks	Initiation Life* Blocks	% Total	Crack Growth Life Blocks	% Total
1	4.1	3.8	93	0.3	7
1	7.3	6.4	87	0.9	13
2	15.3	13.9	91	1.4	9
2	20.1	15.8	79	4.3	21
3	46.8	35.1	75	11.7	25

* Crack length of 1.0 mm from the keyhole notch

LifEst commercial software using the local strain approach with material properties from Tables 2 and 3, rainflow counting, linear damage summation, Neuber (1961) rule or Glinka (1985) rule and the Morrow or SWT mean stress model was used for fatigue crack initiation block life calculations. This required four different solution procedures and four different results for each of the three peak load levels. All these calculations were non-conservative by factors of 1.5 to 5. About half the calculations were within a factor of 2 of the experimental life and the best calculations were achieved using the Morrow mean stress model and Glinka's rule.

To calculate the variable amplitude fatigue crack growth life, LEFM-based non-interaction software using LifEst and NASA/Flagro, computer programs were used. These crack growth programs use the correlation between fatigue crack growth per cycle (da/dN) and stress intensity factor range (ΔK), along with material property data from Table 4. They do not incorporate crack retardation effects. Two crack closure models available with the LifEst software were used in the crack growth life calculations. The first model assumes that crack opening occurs as the loading passes through zero from compression to tension. The stress intensity factor range, therefore, is calculated using positive values in the load or

stress history. The second model assumes a constant "average" opening stress level greater than zero and is determined from the ratio of the minimum and maximum data points in the variable amplitude load history. The NASA/Flagro computer program uses a modified Forman equation for the crack growth rate definition. The calculated fatigue crack growth lives using the different models ranged from non-conservative by a factor of 3 to conservative by a factor of 7. About half the calculations were within a factor of 2. Thus the use of these noninteraction models for fatigue crack growth life calculations showed both good and poor correlations.

The total fatigue life of the keyhole specimen was calculated by adding the fatigue crack initiation life calculation results to the corresponding fatigue crack growth life calculation results. Since four different solution procedures were used in the fatigue crack initiation life calculations and three different solution procedures were used in the fatigue crack growth calculations, a total of twelve solution procedures were possible for the total life calculations. All total life calculations were non-conservative since the crack initiation calculations were all non-conservative. The ratio of total calculated lives to experimental lives ranged from about 1.3 to 5 indicating the fatigue life calculation models can provide both acceptable and unacceptable results. The problem, here, however, is that we do not know a priori which model will provide realistic life calculation results. Thus, this research can only conclude that it is possible to use standard life calculation techniques for sand cast magnesium alloys and obtain both reasonable and unreasonable results.

CONCLUSIONS

1. The conventional log-log bilinear strain life model was an excellent fit for the fully-reversed low cycle fatigue data. Scatter was much less than is typical for cast metals.
2. Significant mean stress relaxation occurred in the mean strain tests, even for some low strain amplitude tests. The mean strain tests affected the fatigue life only if accompanied by mean stress.
3. Both the Morrow and SWT mean stress models described the constant amplitude low cycle fatigue data in a non-conservative manner.
4. Constant amplitude fatigue crack growth data indicated R ratio effects were only partially eliminated by using ΔK_{eff}.
5. Overall, it is shown that, using typical commercially available fatigue life calculation software packages, both fairly accurate and inaccurate fatigue life calculation results for either crack "initiation" or crack growth can be obtained for this AZ91E-T6 sand cast magnesium alloy.

REFERENCES

Elber, W. (1971), "The Significance of Fatigue Crack Closure," Damage Tolerance in Aircraft Structures, STP 486, ASTM, pp. 230-247.

Glinka, G. (1985), "Energy Density Approach to Calculation of Inelastic Strain-Stress Near Notches and Cracks," Engineering Fracture Mechanics, Vol. 22, No. 3, pp. 485-508.

Graham, J.A. (1968), Editor, Fatigue Design Handbook, Society of Automotive Engineers.

Lease, K.B. and Stephens, R.I. (1991), "Verification of Variable Amplitude Fatigue Life Methodologies for a Cast Aluminum Alloy," SAE, Paper No. 910163.

Neuber, H. (1961), "Theory of Stress Concentration for Shear-Strained Prismatical Bodies with Arbitrary Nonlinear Stress-Strain Laws," Journal of Applied Mechanics, Vol. E28, pp. 544-550.

Ogarevic, V.V. and Stephens, R.I. (1990), "Fatigue of Magnesium Alloys," Annual Review of Materials Science, Vol. 20, pp. 141-177.

Smith, K.N., Watson, P. and Topper, T.M. (1970), "A Stress-Strain Function for the Fatigue of Metals," Journal of Materials, Vol. 5, No. 4, pp. 767-778.